Journal of Engineering Physics and Thermophysics, Vol. 77, No. 4, 2004

THERMODYNAMIC AND KINETIC THEORY OF TRANSFER PROCESSES

MODELING IN POLYSECTIONED THERMODYNAMIC SYSTEMS

D. B. Volov

UDC 517.958:531.332

A single algorithm for calculating thermodynamic systems whose volume is limited by a finite number of facility elements is constructed. Having a unified model at one's disposal, it is possible to construct on its basis mathematical models for specific structures. Practical examples of the realization of this approach in ballistic compressors are considered.

Introduction. There are many gas-dynamic problems in solving which it is enough to restrict oneself to the thermodynamics. Among them are the majority of problems on modeling the operation of ballistic devices used in scientific investigations on plasma- and photochemistry, for pumping solid-state lasers, etc. [1–3].

Considering the mathematical models constructed for specific facilities of such a kind [4, 5]. it can easily be seen that with increasing number of elements (pistons, diaphragms, valves) and parameters taken into account in the calculation, the complexity of obtaining the input system of equations sharply increases. In actual fact, only the problems for elementary systems (a single-piston plasmatron with a diaphragm, a trunk system, simplified problems of multi-stage compression, etc.) have been solved.

Now that a fairly large amount of experimental data on the operation of ballistic plasmatrons and similar devices is available [4–7], the necessity of constructing a single algorithm for determining the thermal-energy characteristics of gas and calculating the piston dynamics has arisen. The proposed scheme generalizing the experience of the models used in practice fulfills these purposes.

Having a unified model at our disposal, we can both construct on its basis mathematical models for particular structures and elucidate the most general principles and laws inherent in all systems of this kind on the whole.

Problem Formulation. We have a thermodynamic system whose volume is limited by a finite number of facility elements, with individual parts of this system interacting with one another. The mechanisms of such a coupling can be quite different: heat and mass transfer through the nozzle parts of the devices, radiation heat exchange, heat conduction through the walls, change in the state of the working-substance parameters due to the motion of the walls (pistons), and so on. It is required to construct a mathematical model for calculating the operation dynamics and the thermodynamic characteristics at each internal point of the device.

The calculations and experimental data show [5, 7] that such systems can be split into so-called sections — parts of the space bounded by the walls — and the gas parameters in them can be assumed to be equal at all points at a fixed instant of time. Each section has J inlets and outlets, the section walls are movable and permeable to radio radiation, heat conduction, and other kinds of energy transfer (Fig. 1), and the interaction thereby is realized both between sections and with the environment. Therefore, in the presence of the heat exchange with the environment, it is expedient to designate this environment as section 0.

The principle of splitting into sections can be extended to any gas thermodynamic systems where the following conditions are met:

1) the gas parameters are equal inside a separated section and the rate of their change is much lower than the disturbance propagation velocity in the section;

T. M. Elizarov Samara Institute of Railway Engineers, 18 1st Bezymyannyi lane, Samara, 443066, Russia; email: volovdm@mail.ru. Translated from Inzhenerno-Fizicheskii Zhurnal, Vol. 77, No. 4, pp. 132–143, July–August, 2004. Original article submitted September 10, 2003.

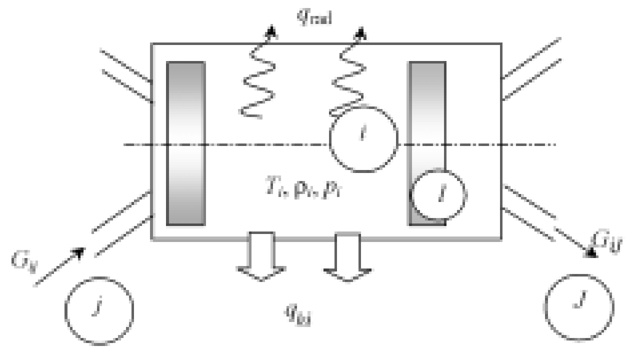

Fig. 1. Arbitrary section of the facility.

2) the characteristic times of the intersection processes are much larger than the time of the sound wave passage between sections.

Construction of a Mathematical Model. As working media, we will consider gases with known equations of state. For the sake of simplicity, we restrict ourselves to the case of a perfect gas, which will not affect the essence and generality of the method. The change in the gas parameters in an individual section is described by a system expressing the mass and energy conservation laws [8]. Let us write the equations for an arbitrary ith section:

$$\frac{dm_i}{dt} = \sum_j G_{ij} + \sum_k g_{ki}\,, \tag{1}$$

$$\frac{d\,(m_i c_{Vi} T_i)}{dt} + p_i \frac{dV_i}{dt} = \sum_j H_{ij} G_{ij} + \sum_k q_{ki}\,. \tag{2}$$

Subscripts ij indicate the heat and mass exchange between the ith and the other sections through the jth hole. The gas flow through the chosen area Ξ is

$$G = \int_S \rho \mathbf{w} \cdot d\Xi\,.$$

The gas can flow into a section from other sections with high pressures and flow out into sections with low pressures. To preserve a single-solution algorithm, for the gas flow between sections, we should write the gas flow rate [8] as

$$G_{ml} = -S_{ml}\rho_m a_{ml} \begin{cases} \left(\dfrac{2}{\gamma_m + 1}\right)^{\frac{\gamma_m+1}{2(\gamma_m-1)}}, & p_l < p_m k_m\,; \\ \sqrt{\dfrac{2}{\gamma_m - 1}\left(1 - \left(\dfrac{p_l}{p_m}\right)^{\frac{\gamma_m-1}{\gamma_m}}\right)} \left(\dfrac{p_l}{p_m}\right)^{\frac{1}{\gamma_m}}, & p_m k_m \le p_l < p_m\,; \end{cases} \tag{3}$$

$$k_m = \left(1 - \frac{\gamma_m - 1}{\gamma_m + 1}\right)^{\frac{\gamma_m}{\gamma_m-1}}, \quad a_{ml} = \frac{p_m - p_l}{|p_m - p_l|}\sqrt{\gamma_m \frac{R_0}{\mu_m} T_m}\,, \quad m, l = \begin{cases} i, j, & p_i > p_j\,; \\ j, i, & p_i \le p_j\,. \end{cases}$$

The use of the module operator in the formula for the second velocity a_{ml} permits taking into account the directions of the gas flow.

Let us split the ith-section surface σ_i into elementary walls with area $d\mathbf{S}_i = \mathbf{n}_i dS_i$ and draw a radius vector $\mathbf{r}_i$ to each of them. Then the gas volume is

$$V_i = \frac{1}{3} \iint_{\sigma_i} \mathbf{r} \cdot d\mathbf{S}\,, \tag{4}$$

which follows, e.g., from the Ostrogradskii–Gauss formula. The section walls can change their position in the space, as a result of which the volume of the section as a whole will change. Each radius vector points to an elementary mass dm_i, whose equation of motion is

$$dm_i \ddot{\mathbf{r}}_i = \sum_j (d\mathbf{F}_i)_j + \sum (d\mathbf{F}_i)^{\text{in}} + \sum_j (d\mathbf{F}_i)^*_{k-j}\,.$$

If by external forces we mean pressure forces, then

$$dF_{ij} = p_i d\sigma_{ij} - p_j d\sigma_{ji}\,.$$

In problems with moving pistons, the wall coordinates change only along a certain x axis. This takes place, e.g., when the piston wall is moving along the trunk axis. Then integral (4) can be given in the form

$$V_i\,(t) = \int_{A(t)}^{B(t)} S_i\,(x, t)\,dx\,,$$

where $A(t)$ and $B(t)$ are found from the equations of motion.

In this case, the walls with coordinates A and B defining the boundaries of V_i represent solid bodies with masses

$$\int_{m_A} dm_i = m_A\,, \quad \int_{m_B} dm_i = m_B\,,$$

so that the internal forces compensate for one another, and the equation of motion of the lth wall-piston ($l = A$, $l = B$, ...) is

$$m_{\text{pl}} \frac{d^2 x_l}{dt^2} = \sum_j F_{lj} + \sum_k F^*_{lk}\,. \tag{5}$$

It is convenient to solve system (1), (2), (5) in the variables T, ρ, and V ($x = x(V)$):

$$V_i\,(t) = \int_{x_l} S_i\,(x, t)\,dx\,, \tag{6}$$

$$\frac{d\rho_i}{dt} = \frac{1}{V_i} \sum_j G_{ml} - \frac{\rho_i}{V_i}\frac{dV_i}{dt} + \frac{1}{V_i} \sum_k g_{ki}\,, \tag{7}$$

$$\frac{dT_i}{dt} = \frac{1}{V_i} \sum_j \left[\frac{1}{\rho_i}\left(\frac{c_{pm}}{c_{Vi}} T_m - T_i\right) G_{ml}\right] - (\gamma_i - 1)\,\frac{T_i}{V_i}\frac{dV_i}{dt} - \frac{1}{c_{Vi}\rho_i V_i} \sum_k q_{ki}\,, \tag{8}$$

where G_{ml} is determined by formula (3). The system is closed by the equations of state of the gas. The transition from the heat capacities of gases c_{pi} and c_{V_i} to their adiabatic indices γ_i and molar masses μ_i for a perfect gas is realized with regard for the Mayer equation [8].

The system of equations (6)–(8) can be written in the matrix form

$$\frac{d}{dt}\left[\mathbf{M}, \mathbf{E}, \overline{\mathbf{x}}, \mathbf{m}_{\mathrm{p}} \frac{d\overline{\mathbf{x}}}{dt}\right] = \left[\mathbf{S}{*}\rho\mathbf{u}, \mathbf{S}{*}(\mathbf{c}_p\mathbf{T}\rho\mathbf{u}), \frac{d\overline{\mathbf{x}}}{dt}, \overline{\boldsymbol{\sigma}\cdot\mathbf{p}}\right] + \mathbf{Q}\,, \tag{9}$$

where the column vectors

$$\mathbf{M} = \begin{bmatrix} \rho_1 V_1 \\ \rho_2 V_2 \\ \ldots\ldots \\ \rho_N V_N \end{bmatrix}, \quad \mathbf{E} = \begin{bmatrix} c_{V1}\rho_1 T_1 V_1 \\ c_{V2}\rho_2 T_2 V_2 \\ \ldots\ldots\ldots\ldots \\ c_{VN}\rho_N T_N V_N \end{bmatrix}, \quad \overline{\mathbf{x}} = \begin{bmatrix} \overline{x}_1 \\ \overline{x}_2 \\ \ldots \\ \overline{x}_N \end{bmatrix}, \quad \rho\mathbf{u} = \begin{bmatrix} \rho_1 u_1 \\ \rho_2 u_2 \\ \ldots\ldots \\ \rho_N u_N \end{bmatrix}, \quad \mathbf{c}_p\mathbf{T}\rho\mathbf{u} = \begin{bmatrix} c_{p1} T_1 \rho_1 u_1 \\ c_{p2} T_2 \rho_2 u_2 \\ \ldots\ldots\ldots\ldots \\ c_{pN} T_N \rho_N u_N \end{bmatrix},$$

$$\mathbf{p} = \begin{bmatrix} p_1 \\ p_2 \\ \ldots \\ p_N \end{bmatrix}, \quad \mathbf{S} = \begin{bmatrix} S_{11} S_{12} \ldots S_{1N} \\ S_{21} S_{22} \ldots S_{2N} \\ \ldots\ldots\ldots\ldots\ldots \\ S_{N1} S_{N2} \ldots S_{NN} \end{bmatrix}, \quad \boldsymbol{\sigma} = \begin{bmatrix} \sigma_{11}\sigma_{12} \ldots \sigma_{1N} \\ \ldots\ldots\ldots\ldots\ldots \\ \sigma_{l1}\sigma_{l2} \ldots \sigma_{lN} \end{bmatrix}, \quad \mathbf{Q} = \begin{bmatrix} g_1, q_1, 0, \overline{F}_1^* \\ g_2, q_2, 0, \overline{F}_2^* \\ \ldots\ldots\ldots\ldots\ldots \\ g_N, q_N, 0, \overline{F}_N^* \end{bmatrix}.$$

The bar over the factor indicates that multiplication of matrices yields vector equations which should be expanded in projections.

The solution of this system at given initial conditions is the time-dependent macrostate matrix

$$\left[\rho, \mathbf{T}, \frac{d\mathbf{V}}{dt}, \mathbf{V}\right] = \begin{bmatrix} \rho_1 T_1 \dfrac{dV_1}{dt} V_1 \\ \rho_2 T_2 \dfrac{dV_2}{dt} V_2 \\ \ldots\ldots\ldots\ldots\ldots \\ \rho_N T_N \dfrac{dV_N}{dt} V_N \end{bmatrix}.$$

In formula (9), by the sign * is meant the operand of the so-called conditional multiplication, whose rules are analogous to the rules of multiplication of matrices with the difference being that for each nonzero term one also considers the additional conditions determined for the antisymmetric term. In general, for two matrices **A** and **B** the conditional multiplication should be understood to be such that the result of their multiplication is the matrix **C** ($\mathbf{A}{*}\mathbf{B} = \mathbf{C}$) each term of which c_i is calculated according to the rule

$$c_i = \sum_{j=1}^{n} \begin{cases} a_{ij} b_j\,, & p_j > p_i\,; \\ -\,a_{ji} b_i\,, & p_j \le p_i\,, \end{cases}$$

where the condition has been determined by some feature **P** (in the present paper, by the section pressure). Detailed explanations concerning the use of the matrix notation (9) will be given in example No. 2 in the next section.

System (9) gives

$$u_i = \sqrt{\gamma_i \frac{R_0}{\mu_i} T_i} \begin{cases} \left(\dfrac{2}{\gamma_i + 1}\right)^{\frac{\gamma_i+1}{2(\gamma_i-1)}}, & p_j < p_i k_i\,, \quad k_i = \left(1 - \dfrac{\gamma_i - 1}{\gamma_i + 1}\right)^{\frac{\gamma_i}{\gamma_i-1}}\,; \\ \sqrt{\dfrac{2}{\gamma_i - 1}\left(1 - \left(\dfrac{p_j}{p_i}\right)^{\frac{\gamma_i-1}{\gamma_i}}\right)} \left(\dfrac{p_j}{p_i}\right)^{\frac{1}{\gamma_i}}, & p_i k_i \le p_j < p_i\,. \end{cases}$$

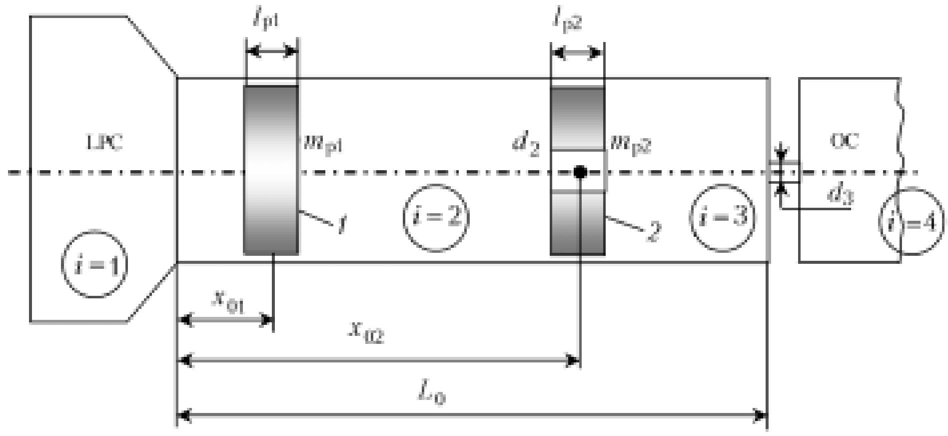

Fig. 2. Scheme of the two-stage plasmatron.

The cross-section matrix components **S** in (9) are symmetric ($S_{ij} = S_{ji}$) if there are no additional devices influencing the flow from the ith section to the jth section when the direction of the process is changed (valves, nozzles with a variable cross section, etc.).

The macrostate matrix may not be restricted to the parameters T, ρ, and $V(x, dx/dt, \sigma)$ but can also incorporate other quantities: flow fields, electric and magnetic field strengths, degrees of ionization, etc. However, exchange matrices, **S**, σ, and others, as well as matrices (9) in the conditional multiplication are always coupled. For example, if we take into account the heat transfer W_i through the section walls, then a coupled matrix σ^* will appear:

$$W_i = \alpha\sigma^* (T_i - T_0) .$$

Practical Application of the Proposed Model and Its Realization. Despite the standard general form of the initial system of equations (9), specific examples of its realization in mathematical models are diverse. We will highlight two of them.

Example No. 1. Two-stage ballistic plasmatron. Consider the obtained system (6)–(8) as applied to the two-stage ballistic plasmatron (Fig. 2) [3]. It may be considered that initially the low-pressure chamber (LPC) contained a driver gas (air) at some pressure p_{01} (up to 2 Pa) (the LPC will be considered in detail in example No. 2).

In the given device, there is practically no exchange with the environment; therefore, the 0th section is excluded. Here zero is used to designate the initial conditions.

The initial positions of the heavy piston 1 and the light piston 2 (Fig. 2) are rigidly fixed. The light piston has a cross-over nozzle of diameter d_2, and the gas is blown into the outlet chamber through a nozzle of diameter d_3. The plasmatron trunk contains the working gas at some pressure. The two-piston system permits obtaining higher temperatures at lower pressures compared to the adiabatic single-piston compression [2, 3].

When the driver gas gets into the plasmatron trunk, the heavy piston comes into motion, compressing the working gas. As experiments show [7], the light piston, as a consequence of inertia, remains practically stationary until the heavy piston approaches it. As this takes place, the gas flows from the space between the pistons to the region behind the second piston. Then the gas is recompressed by both pistons.

It is necessary to calculate the characteristics of the working gas (temperature, pressure, density) in the process of compression and determine the laws of motion of the pistons.

We distinguish four sections (Fig. 2): 1 — LPC, 2 — between the first and second pistons, 3 — after the second piston of the plasmatron, and 4 — outlet chamber (OC). There are two movable walls-pistons (l = 2).

To construct a mathematical model of the device, we make use of relations (6)–(8), taking into account (3). The cross-section areas of the nozzles are: $S_1 = 0$; $S_2 = \pi d_2^2/4$; $S_3 = \pi d_3^2/4$; and $S_4 = 0$. The cross-section areas of the sections are constant and equal to $\sigma = \pi D^2/4$. We ignore the chemical processes ($g_{ki} = 0$, $\forall\ i, k$) and calculate the radiation loss q_{ki} by the computational procedure of [9]. The other heat transfer processes (heat transfer through the walls, convective heat exchange) play an insignificant role here, since the pulse durations are rather small.

TABLE 1. Input Data for Calculating the BP-2 Ballistic Plasmatron

D, m	d_2, m	d_3, m	x_{01}, m	x_{02}, m	L_0, m	l_{p1}, m	l_{p2}, m	V_{01}, m^3	V_4, m^3	m_{p1}, kg	m_{p2}, kg
0.076	0.006	0(7)	0.041	0.665	0.84	0.08	0.08	$1.48 \cdot 10^{-3}$	$2 \cdot 10^{-3}$	3.0	1.0

TABLE 2. Initial Parameters of Gas for Calculations (1 and 2, Experiment Numbers)

Section	γ		μ, kg/mole		T_0, K	ρ_0, kg/m^3		$p_0 \cdot 10^5$, Pa	
	1	2	1	2		1	2	1	2
1	1.4	1.4	0.028	0.028	300	1.138	1.138	100	100
2	1.4	1.67	0.028	0.131	300	1.138	5.33	1	1
3	1.4	1.67	0.028	0.131	300	1.138	5.33	1	1
4	1.4	1.4	0.028	0.028	300	$1.138 \cdot 10^{-4}$	$1.138 \cdot 10^{-4}$	10^{-4}	10^{-4}

For the first section, the flow rate equation and the energy equation directly integrate (adiabatic processes). As a result, the initial system of equations (6)–(8), (3) is simplified:

$$m_{p1}\frac{d^2x_1}{dt^2}=R_0\frac{\pi D^2}{4}\left[\frac{M_{01}T_{01}\,(V_{01}/V_1)^{\gamma_1-1}}{(V_{01}+(\pi D^2/4)\,(x_1-l_{p1}/2))\mu_1}-\frac{\rho_2T_2}{\mu_2}\right]-F_{fr1}\,,$$

$$m_{p2}\frac{d^2x_2}{dt^2}=R_0\frac{\pi D^2}{4}\left[\frac{\rho_2T_2}{\mu_2}-\frac{\rho_3T_3}{\mu_3}\right]-F_{fr2}\,,$$

$$\frac{d\rho_2}{dt}=\frac{G_{ml}}{V_2}\left(m,l=\begin{cases}2,3,\;p_2>p_3\\3,2,\;p_2\le p_3\end{cases}\right)-\frac{\rho_2}{V_2}\frac{dV_2}{dt}\,,$$

$$\frac{d\rho_3}{dt}=\frac{G_{ml}}{V_3}\left(m,l=\begin{cases}3,2,\;p_3>p_2\\2,3,\;p_3\le p_2\end{cases}\right)+\frac{G_{ml}}{V_3}\left(m,l=\begin{cases}3,4,\;p_3>p_4\\4,3,\;p_3\le p_4\end{cases}\right)-\frac{\rho_3}{V_3}\frac{dV_3}{dt}\,,$$

$$\frac{d\rho_4}{dt}=\frac{G_{ml}}{V_4}\left(m,l=\begin{cases}4,3,\;p_4>p_3\\3,4,\;p_4\le p_3\end{cases}\right),$$

$$\frac{dT_2}{dt}=\frac{G_{ml}}{V_2\rho_2}\left(\frac{c_{pm}}{c_{V2}}T_m-T_2\right)\left(m,l=\begin{cases}2,3,\;p_2>p_3\\3,2,\;p_2\le p_3\end{cases}\right)-(\gamma_2-1)\frac{T_2}{V_2}\frac{dV_2}{dt}-\frac{q_2}{c_{V2}\rho_2V_2}\,,$$

$$\frac{dT_3}{dt}=\frac{G_{ml}}{V_3\rho_3}\left(\frac{c_{pm}}{c_{V3}}T_m-T_3\right)\left(m,l=\begin{cases}3,2,\;p_3>p_2\\2,3,\;p_3\le p_2\end{cases}\right)+\frac{G_{ml}}{V_3\rho_3}\times \tag{10}$$

$$\times\left(\frac{c_{pm}}{c_{V3}}T_m-T_3\right)\left(m,l=\begin{cases}3,4,\;p_3>p_4\\4,3,\;p_3\le p_4\end{cases}\right)-(\gamma_3-1)\frac{T_3}{V_3}\frac{dV_3}{dt}-\frac{q_3}{c_{V3}\rho_3V_3}\,,$$

$$\frac{dT_4}{dt}=\frac{G_{ml}}{V_4\rho_4}\left(\frac{c_{pm}}{c_{V4}}T_m-T_4\right)\left(m,l=\begin{cases}4,3,\;p_4>p_3\\3,4,\;p_4\le p_3\end{cases}\right)-\frac{q_4}{c_{V4}\rho_4V_4}\,,$$

where $V_1 = V_{01}+(\pi D^2/4)(x_1-l_{p1}/2)$; $V_2 = (\pi D^2/4)((x_2-l_{p2}/2)-(x_1+l_{p1}/2))$; $V_3 = (\pi D^2/4)(L_0-(x_2+l_{p2}/2))$; and $V_4 = V_{04}$; the components G_{ml} are calculated by formula (3). For the two-stage plasmatron, a system analogous to (10) was first obtained by V. M. Shmelev and N. Ya. Vasilik (Institute of Physical Chemistry, Moscow) [4].

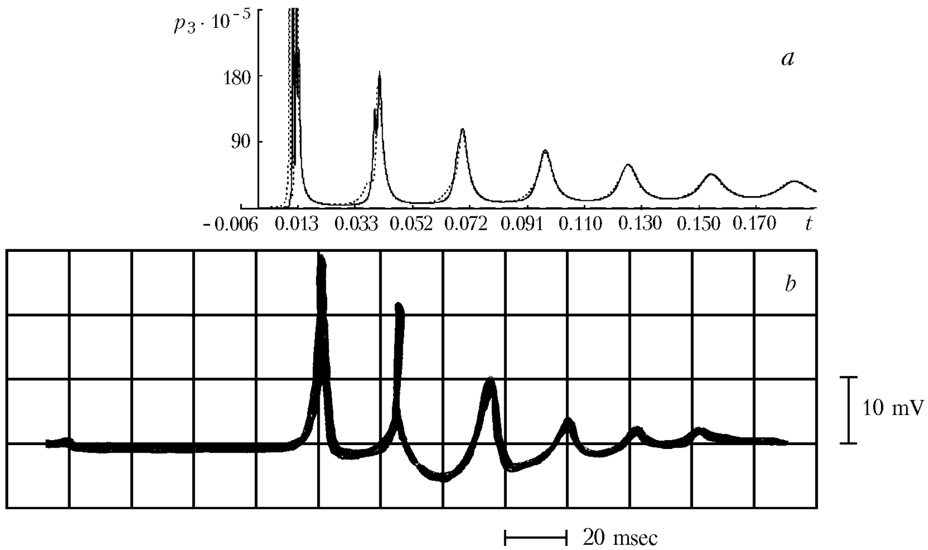

Fig. 3. Pressure p_3 at air compression: a) calculation; b) experimental data.

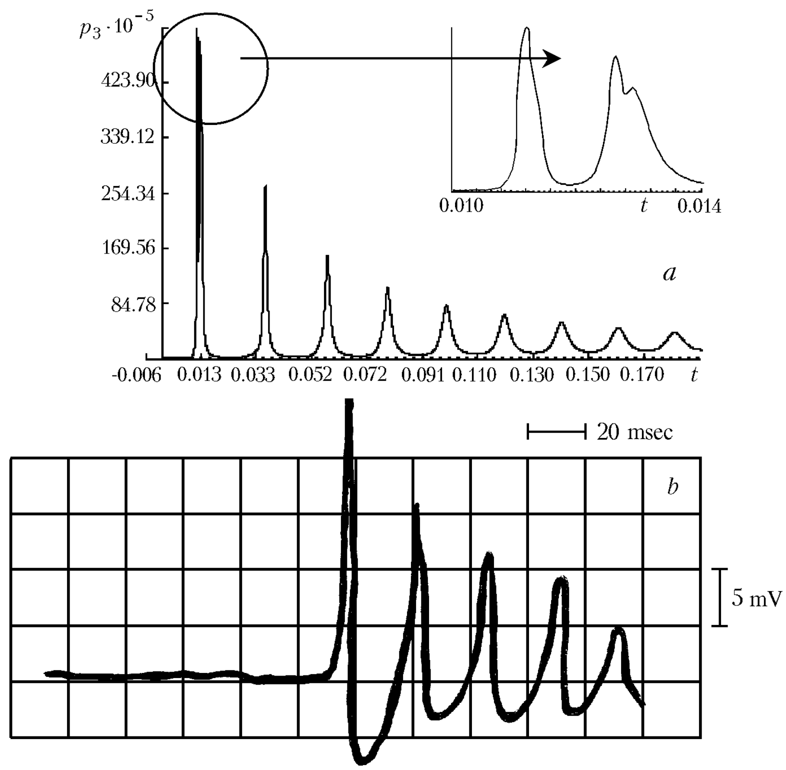

Fig. 4. Pressure p_3 at xenon compression: a) calculation; b) experimental data.

Let us calculate the operating conditions of the two-stage plasmatron, for which experimental studies were made earlier [7], and compare the results. The input data for the calculation are given in Tables 1 and 2.

In the first experiment, the compression process without forcing of the gas out of the plasmatron trunk (d_3 = 0) is considered. The working gas is air. Figure 3a shows the pressure–time diagram for the 3rd section, and Fig. 3b gives the pressure oscillogram for the same working conditions. Comparing these figures, it can be seen that on the time scan the moments at which pulse peaks appear practically completely coincide. The difference between the calculated values of pressures p_3 and the experimental data do not exceed 10.9% (the sensitivity corresponds to $1.47 \cdot 10^6$ Pa per 1 mV). In the experiments, the variable component of the signal was fixed. The ray emergence in the region with

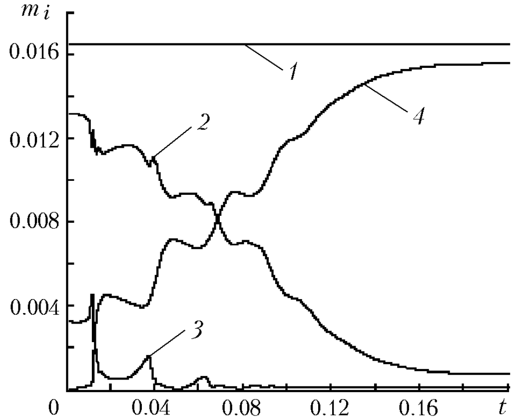

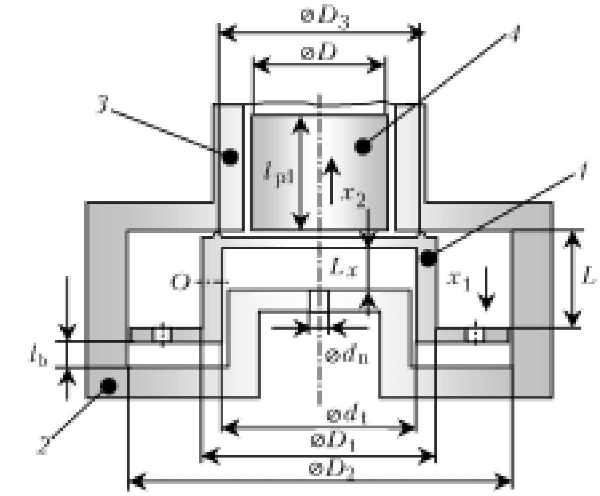

Fig. 5. Mass redistribution between sections in the course of the process (xenon, d_3 = 7 mm): 1) control total mass of gas in sections 2, 3, 4; 2) gas mass in section 2; 3) same in section 3; 4) same in section 4.

Fig. 6. Scheme of the starting device.

negative values is not associated with the physical processes but is explained by the specificity of the oscilloscope operation (capacitor overcharge) [7].

In the second experiment, xenon comparison at d_3 = 0 and 7 mm was modeled. The difference between the obtained values and the experimental data for the pressures in section 3 does not exceed 4.7%. In Fig. 4a, one can discern the fine structure of the first compression impulse, which is unnoticeable on the oscillogram. It also becomes possible to check other parameters that are not measured in the experiments. In Fig. 5, it is seen that at d_3 = 7 mm not all of the working-gas mass is transferred to the 4th section during the first compression impulse. For the plasmatron, the monopulse regime of operation is preferable. In the numerical experiment, selecting the nozzle diameter, one can obtain exactly these operating conditions.

The experimental data were processed for a wide circle of problems in a wide range of temperatures and pressures (up to 15,000 K and $1.3 \cdot 10^8$ Pa) for different kinds of the working substance (air, xenon, argon, helium, mixture of gases). The results obtained permit speaking of calculation accuracies reasonable for engineering calculations (error up to 15%). Modeling of the processes in the two-stage ballistic plasmatron permits gaining a deeper insight into the physics of a process and opens up widespread possibilities for optimizing the facility.

Example No. 2. System for starting the ballistic plasmatron, LPC. Such systems use starting devices, whose basic units are the plate 1 and the bottom of the valve 2, nearest to which is the plasmatron trunk 3 with a piston 4 (Fig. 6). First the driver gas is allowed to bleed into the LPC from the side of the plate bottom. As this takes place, in the low-pressure chamber formed by elements 1 and 2 (Fig. 6) the pressure is the same everywhere because of the gas flow through the hole *O*. The plasmatron is started by an electromagnetic valve with a hole of diameter d_n. Due to the pressure difference, the plate 1 goes down to close the hole *O*, and for the gas a passage with a cross section $S_1 = \pi D_1 x_1$ (usually $D_3 \approx D_1$) is formed. The driver gas from the LPC swiftly flows into the trunk to set the first piston in motion.

We now proceed to the construction of a mathematical model of operation of the device. The following four sections are distinguished:

1) section 0 — environment;
2) section 1 — space under the plate;
3) section 2 — LPC;
4) section 3 — in the trunk volume before the piston.

Let us make use of the matrix form (9) for composing the system. Determine the corresponding matrices

$$\mathbf{M}=\begin{bmatrix} m_0\\ m_1\\ m_2\\ m_3 \end{bmatrix},\quad \mathbf{E}=\begin{bmatrix} E_0\\ E_1\\ E_2\\ E_3 \end{bmatrix},\quad \bar{\mathbf{x}}=\begin{bmatrix} \bar{x}_1\\ \bar{x}_2 \end{bmatrix},\quad \boldsymbol{\rho}\mathbf{u}=\begin{bmatrix} \rho_0 u_0\\ \rho_1 u_1\\ \rho_2 u_2\\ \rho_3 u_3 \end{bmatrix},\quad \mathbf{c}_p\mathbf{T}\boldsymbol{\rho}\mathbf{u}=\begin{bmatrix} c_{p0}T_0\rho_0 u_0\\ c_{p1}T_1\rho_1 u_1\\ c_{p2}T_2\rho_2 u_2\\ c_{p3}T_3\rho_3 u_3 \end{bmatrix},\quad \mathbf{p}=\begin{bmatrix} p_0\\ p_1\\ p_2\\ p_3 \end{bmatrix},$$

$$\mathbf{S}=\begin{bmatrix} 0 & S_n & 0 & 0\\ S_n & 0 & 0 & 0\\ 0 & 0 & 0 & S_1\\ 0 & 0 & S_1 & 0 \end{bmatrix},\quad \boldsymbol{\sigma}=\begin{bmatrix} 0 & S_t & 0 & S_D\\ 0 & 0 & 0 & S_D \end{bmatrix},\quad \mathbf{Q}=\begin{bmatrix} 0\,0\,0\,0\\ 0\,0\,0\,0\\ 0\,0\,0\,0\\ 0\,0\,0\,0 \end{bmatrix}, \tag{11}$$

where $S_n = \pi d_n^2/4$; $S_t = \pi d_t^2/4$; and $S_D = \pi D^2/4$. The matrix $\mathbf{Q}$ turns out to be zero, since under the conditions being considered the mass and energy internal sources are practically absent, and the influence of the friction forces in such a short time of motion can be neglected. The result of the conditional multiplication will be

$$\frac{d\mathbf{M}}{dt}=\mathbf{S}*\boldsymbol{\rho}\mathbf{u}=\begin{bmatrix} \begin{cases} \rho_1 u_1 S_n\,, & p_1 > p_0\,,\\ -\rho_0 u_0 S_n\,, & p_1 \le p_0\,; \end{cases}\\[2ex] \begin{cases} \rho_0 u_0 S_n\,, & p_0 > p_1\,,\\ -\rho_1 u_1 S_n\,, & p_0 \le p_1\,; \end{cases}\\[2ex] \begin{cases} \rho_3 u_3 S_1\,, & p_3 > p_2\,,\\ -\rho_2 u_2 S_1\,, & p_3 \le p_2\,; \end{cases}\\[2ex] \begin{cases} \rho_2 u_2 S_1\,, & p_2 > p_3\,,\\ -\rho_3 u_3 S_1\,, & p_2 \le p_3 \end{cases} \end{bmatrix}.$$

An analogous expression is obtained for $d\mathbf{E}/dt$.

Since we have two moving walls, $l = 2$. Let us draw the x_1 and x_2 axes in the direction of the supposed motion of the plate and the piston, respectively (Fig. 6). Consequently, the equations for the velocities of motion $d\bar{\mathbf{x}}/dt = \bar{\mathbf{w}}$ in the projections on these axes are $dx_1/dt = w_1$ and $dx_2/dt = w_2$.

We will consider that the working gas at the beginning of the compression stage does not influence the piston dynamics. In actual fact, the pressure forces of the working gas at this instant are two orders of magnitude smaller than the driver-gas forces and they can be neglected. In such a situation, in writing the equation of motion of the piston, it is enough to restrict ourselves to the consideration of the influence of one force, $[\boldsymbol{\sigma}\cdot\mathbf{p}]_{23} = p_1\pi D^2/4$. Therefore, the same $\boldsymbol{\sigma}$ matrix as in (11) is obtained.

Multiplying $\boldsymbol{\sigma}\cdot\mathbf{p}$ in accordance with (9) leads to the vector equations

$$\frac{d}{dt}\left(m_{p1}\frac{d\bar{x}_1}{dt}\right)=\overline{p_1 S_t}+\overline{p_3 S_D}\,,\quad \frac{d}{dt}\left(m_{p2}\frac{d\bar{x}_2}{dt}\right)=\overline{p_3 S_D}\,,$$

whose projections on the given directions x_1 and x_2 will be present in the sought system of equations.

In principle, at this point the model of the LPC operation can be considered to be constructed and we can proceed with integrating the system of equations obtained. In this case, the problem solution can be simplified, taking into consideration the direction of the processes: in the time interval under consideration, $p_0 < p_1$ and $p_3 < p_2$. Since the temperature in the process varies within the limits of $\Delta T_i < 200$ K, we have $\gamma_0 = \gamma_1 = \gamma_2 = \gamma_3 = \gamma$ and the physical properties of the gas in different sections are the same. We consider the gas to be perfect. The pressure difference between the sections quickly passes the critical mark and, therefore, we assume that the outflow rate is equal to the velocity of sound in the critical cross section:

TABLE 3. Starting Device Characteristics (linear sizes are given in millimeters)

D	D_1	D_2	D_3	d_t	d_n	L_1	L_x	l_b	m_{p1}, kg	m_{p2}, kg
76	146	194	116	122	14	94	20	14	7.60	2.83

$$u_i = \sqrt{\gamma \frac{R_0}{\mu_i} T_i} \left(\frac{2}{\gamma + 1}\right)^{\frac{\gamma+1}{2(\gamma-1)}} = a_i\,, \quad \forall i = \overline{0, 3}\,.$$

We assume that the environment (section 0) has an unlimited store of energy and mass of the gas (dm_0/dt = 0 and dE_0/dt = 0). In the absence of mass sources the number of differential equations in the system can be decreased. To this end, it is enough to express, e.g., the mass m_3 in terms of the gas masses in the other sections.

On the basis of the foregoing, the operation of the starting device can be described by the following system of differential equations:

$$m_{p1} \frac{d^2 x_1}{dt^2} = \frac{R_0}{\mu} \left(\frac{T_3 m_3}{x_1 + (D/D_1)^2 x_2} - \frac{T_1 m_1 (t)}{L_x - x_1} \right), \quad m_{p2} \frac{d^2 x_2}{dt^2} = \frac{R_0}{\mu} \left(\frac{T_3 m_3}{(D_1/D_1)^2 x_1 + x_2} \right),$$

$$\frac{dm_1}{dt} = -\frac{m_1}{L_x - x_1} a \left(\frac{d_n}{d_t}\right)^2, \quad \frac{dm_2}{dt} = -\frac{m_2}{V_2} aS_1\,, \quad m_3 = m_{03} + m_{02} - m_2 (t)\,,$$

$$\frac{dT_1}{dt} = -(\gamma - 1)\frac{T_1}{V_1}\left(\frac{dV_1}{dt} + aS_n\right), \quad \frac{dT_2}{dt} = -(\gamma - 1)\frac{T_2}{V_2}\left(\frac{dV_2}{dt} + aS_1\right), \tag{12}$$

$$\frac{dT_3}{dt} = \frac{aS_1}{V_2}\frac{m_2}{m_3}(\gamma T_2 - T_3) - (\gamma - 1)\frac{T_3}{V_3}\frac{dV_3}{dt}\,,$$

where $V_1 = \pi(L_x - x_1)d_t^2/4$; $V_2 = \pi l_b(D_2^2 - d_t^2)/4 + \pi L_1(D_2^2 - D_1^2)/4$; and $V_3 = \pi x_1 D_1^2/4 + \pi x_2 D^2/4$.

Let us perform calculations for the starting device used in the BP2 ballistic plasmatron (Institute of Chemical Physics, Russian Academy of Sciences). Its characteristics are given in Table 3.

Solving system (12) by numerical methods, it has been obtained that the process of shifting the plate to the extreme lower position takes 1.3 msec. During this time the piston manages to travel a distance of x_2 = 0.0116 m, which is comparable to the pass of the plate itself (l_b = 0.014 m).

The curves of the change in the pressures in the LPC, in the trunk, and under the plate are given in Fig. 7. It is seen that at the beginning of the plate motion the gas pressure in the trunk rapidly (during t = 1.3 msec) increases (Fig. 7, curve 3), approaching the LPC pressure (point A). The kink (point B) corresponds to the moment the plate contacts the plasmatron bottom. In the plot, at t = 0.027 sec one can see a slight short-time increase in the pressure under the plate (point C) due to the compression by the gas from the LPC.

Because of the flow through the "nozzle" of area $\pi D_1 x_1(t)$, the gas temperature in the trunk T_3 (Fig. 8) at the first stage is even higher than the initial temperature ($T_{3\max}$ = 406 K), but with further expansion it decreases even faster than the LPC temperature. This is due to the fact that beginning at some instant of time the process of gas expansion prevails over the process of gas inflow from the LPC. The gas temperature in the LPC (Fig. 8, curve 2) decreases not only because of the expansion but also due to the gas-dynamic cooling in flowing out of the "nozzle." For comparison, Figure 8 gives the curve of the temperature change at adiabatic expansion ignoring the flow and, consequently, the difference in temperatures T_2 and T_3. The maximum value of T_3 is attained at that instant of time when the gas mass m_3 is still small, and this short-time increase in the temperature has no marked effect on the operation dynamics of the device. Subsequently, the deviation of temperatures T_2 and T_3 from the adiabatic temperature T_{ad} is no more than 4%, so that in engineering calculations this process can be considered as adiabatic expansion from a reservoir of volume $V_2 + V_3$.

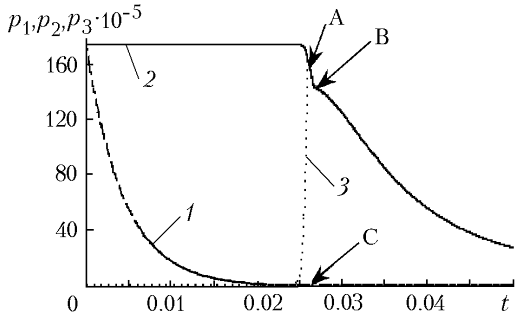

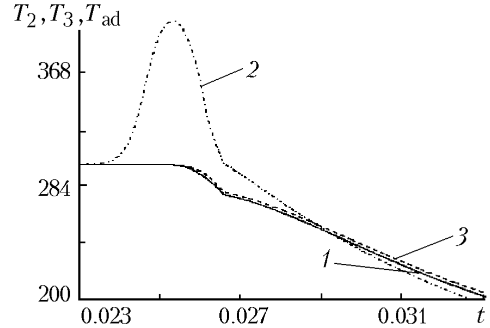

Fig. 7. Pressure variation under the plate (1), in the LPC (2), and in the trunk (3).

Fig. 8. Gas temperatures in the LPC (1), in the trunk (2), and at adiabatic expansion (3).

As the calculations have shown, the nozzle diameter $d_{\rm n}$ influences not only the delay time of the start of motion of the plate.

Let us make relevant analytical estimates. The starting time of the main valve is determined by the ratio between the pressure forces in the trunk (initially equal to the atmospheric pressure) and the pressure forces under the plate. However, since the plate motion causes an additional increase in the pressure and temperature in the outflow, it makes sense to perform calculations in terms of the gas density. Then from the gas-flow equation we determine the time before the start of plate motion as

$$t_{\rm d} = \left(\frac{d_{\rm t}}{d_{\rm n}}\right)^2 \frac{L_x}{a} \ln\left(\frac{\rho_{01}}{\rho_{H1}}\right).$$

For the device under consideration, the deviation from the numerical calculations by $t_{\rm d}$ is 0.90%. In time τ, the piston manages to travel a distance comparable to the pass of the plate ($x_2(\tau)$ = 0.0116 m for the given geometry). As was proposed previously, we represent the process of gas flow from the LPC and its expansion in the trunk by the adiabatic expansion in the volume $V_2 + V_3(\tau)$:

$$p_{\rm ad}(\tau) = p_{02}\left(\frac{V_2}{V_2 + V_3(\tau)}\right)^{\gamma}, \quad V_3(\tau) = x_2(\tau)\,\frac{\pi D^2}{4} \approx \frac{\pi D^2}{4}\, l_{\rm b}\,. \tag{13}$$

According to (13), $p_{\rm ad}(\tau) = 1.29 \cdot 10^7$ Pa, which is 1.8% lower than the calculated one. The corresponding temperature $T_{\rm ad}(\tau)$ = 280 K, although the calculated temperature is 297 K. As mentioned above, this is due to the fact that besides the adiabatic expansion leading to a decrease in the temperature, the nonisotropic gas flow increasing the temperature also plays a role in this process.

Thus, in engineering calculations accurate up to 5% the whole starting process can be replaced by the adiabatic process of gas expansion to the piston position approximately equal to the pass of the plate. The entire process takes time $t = t_{\rm d} + \tau$. Integration of system (12) becomes unnecessary, as a rule, but with its help one can always evaluate the scale of deviations and accuracy of calculations. On the whole, it is enough to restrict oneself to formulas (13), which proves the correctness of the assumption about the LPC made in the first example.

Further calculations for the plasmatron can be started with the moment the plate contacts its bottom, using, as the initial conditions, either numerical or approximate analytical calculations.

Drawing preliminary conclusions, we note that the matrix form of writing used in this example initially takes into account all variants of the course of the processes. And simplification of the system occurs at the stage of elucidation of the features of the problem formulated.

System (6)–(9) is reduced to a system of first-order differential equations by introducing L variables $w_{li} = dx_{li}/dt$ ($l = \overline{1, L}$). Thus, for a device consisting of N sections we have $2(N + L)$ nonlinear first-order equations. They become dimensionless if we assign the variables to their initial values, e.g., in section 1. For such systems the Cauchy theorem holds [10]. Analysis of this system permits the conclusion that a solution of (6)–(9) exists and is unique up to the moment when the volume of one of the sections becomes equal to 0 ($V_i = 0$) (or if the same happens to the gas density ($p_i = 0$)). Using also the dynamic equation of impact, one can obtain unique solutions throughout the time interval under investigation.

CONCLUSIONS

The proposed approach based on splitting into sections is acceptable for calculating a whole class of multistage devices. It permits constructing particular models, using a single mathematical algorithm. The advantages of such an approach are the more pronounced, the more complicated the system (the larger the number of components and units in the structure). The obtained results on the existence and uniqueness of a general system of equations are valid for a whole class of thermodynamic models of technical devices.

NOTATION

$\mathbf{A}$, arbitrary matrix; a, velocity of sound, m/sec; a_i, velocity of sound in the ith section, m/sec; a_{ml}, velocity of sound in the nozzle of transition from the mth to the lth section, m/sec; a_{ij} and a_{ji}, matrix $\mathbf{A}$ components; $A(t)$ and $B(t)$, limits of integration; $\mathbf{B}$, arbitrary matrix; b_i and b_j, components of matrix $\mathbf{B}$; $\mathbf{C}$, arbitrary matrix; $\mathbf{c}_p$, heat matrix of gases; c_i, matrix $\mathbf{C}$ components; c_{pi} and c_{pm}, specific heats of gas at a constant pressure in the ith and mth sections, J/(kg·K); c_{Vi}, specific heat of gas at a constant volume in the ith section, J/(kg·K); D, piston diameter, m; D_1, outside diameter of the plate, m; D_2, inside diameter of the LPC, m; D_3, channel diameter, m; d_2, diameter of the cross-over nozzle in the light piston, m; d_3, diameter of the outlet chamber nozzle, m; d_{n}, diameter of the valve port, m; d_{t}, inside diameter of the plate, m; dF_{ij}, projection of external forces acting on an element of dm_i, N; $(d\mathbf{F}_i)^*_{k-j}$, nonconservative forces arising inside the element, N; $(d\mathbf{F}_i)^{\text{in}}$, interaction forces between wall elements, N; $(d\mathbf{F}_i)_j$, external forces acting on an element of dm_i, N; dm_i, elementary mass, kg; dSi, elementary wall area, m^2; $\mathbf{E}$, energy matrix of gases; E, energy, J; E_0, energy in the 0th section, J; F^*_{lk}, external nonconservative forces in the wall, N; F_{fr1} and F_{fr2}, trunk friction forces of the first and second pistons, N; F_{ij}, projections of forces acting on elements of the wall l from the side of other sections, N; G, gas flow rate, kg/sec; G_{ij} and G_{iJ}, gas flow rate in the ith section through the jth and Jth ports, kg/sec; G_{ml}, gas flow rate in the mth section through the lth port, kg/sec; g_{ki}, powers of the kth sources of mass in the ith section, kg/sec; H_{ij}, specific enthalpy, J/kg; J, total number of inlets and outlets in a section; k_m, critical pressure ratio for the mth section; L, number of first-order equations; L_0, length of the working part of the plasmatron trunk, m; L_1, height of the plate, m; L_x, plate pass (along the x axis), m; l, wall-piston number; l_{p1} and l_{p2}, lengths of the first and second pistons, m; l_{b}, gap width, m; $\mathbf{M}$, matrix of gas masses; $\mathbf{m}_{\text{p}}$, matrix of piston masses; M_{01}, constant mass of gas in the 1st section, kg; m_{02} and m_{03}, initial masses of gas in the 2nd and 3rd sections, kg; m_0, m_1, m_2, and m_3, gas mass in the 0th, 1st, 2nd, and 3rd sections, kg; m_A and m_B, masses of walls A and B; m_i, gas mass in the ith section, kg; $m_{\text{p}l}$, masses of pistons forming a section wall, kg; m_{p1} and m_{p2}, masses of the 1st and 2nd pistons, kg; N, number of sections; $\mathbf{n}_i$, normal to the surface; $\mathbf{P}$, sign matrix; $\mathbf{p}$, pressure matrix; p_0, initial pressure of gas, Pa; p_{01}, initial pressure in the 1st section, Pa; p_1, p_2, p_3, and p_4, gas pressures in the 1st, 2nd, 3rd, and 4th sections, Pa; p_{ad}, pressure corresponding to the adiabatic process, Pa; p_i, p_j, p_l, and p_m, gas pressures in the ith, jth, lth, and mth sections, Pa; $\mathbf{Q}$, disturbance matrix; q_{ki}, powers of the kth energy sources in the ith section, W; q_{rad}, powers of radiation losses, W; $\mathbf{r}$, radius vector; $\ddot{\mathbf{r}}$, second time derivative of the radius vector; $\mathbf{r}_i$, radius vector for the ith section; R_0, universal gas constant, J/(mole·K); $\mathbf{S}$, nozzle section matrix; S, port area, m^2; S_1, S_2, S_3, and S_4, section areas of the 1st, 2nd, 3rd, and 4th nozzles, m^2; S_i, area of the ith section wall, m^2; S_D, section area of the plasmatron trunk, m^2; S_{ji} and S_{ij}, components of the nozzle section matrix; S_{ml}, nozzle section area in the gas flow from the mth section to the lth section, m^2; S_{t}, section area of the plate, m^2; S_{n}, section area of the valve, m^2; $\mathbf{T}$, temperature matrix; T_0, initial temperature, K; T_{01}, initial temperature in the 1st section, K; T_2, T_3, and T_4, temperatures in the 2nd, 3rd, and 4th sections, K; T_i and T_m, temperatures of gases in the ith and mth sections, K; T_{ad}, temperature in the adiabatic process, K; t, time, sec; t_{d}, time before the start of motion of the plate, sec; $\mathbf{u}$, matrix of gas flow velocities; u, gas flow velocity, m/sec; u_i, matrix $\mathbf{u}$ components; $\mathbf{V}$, volume matrix; V_{01} and V_{04}, initial volumes of the 1st and 4th sections;

V_i, gas volume in the ith section, m^3; **w**, velocity vector; W_i, power of heat transfer through the walls, W; w_1 and w_2, velocities of the 1st and 2nd walls, m/sec; w_{li}, velocity of the lth wall of the ith section, m/sec; $\bar{\mathbf{x}}$, displacement vector matrix; $\bar{x}$, wall displacement vectors; $\bar{x}_1$ and $\bar{x}_2$, displacement vectors of the 1st and 2nd walls; x, coordinate axis; x_{01} and x_{02}, initial coordinates of the 1st and 2nd walls, m; x_1 and x_2, coordinates of the 1st and 2nd walls, m; x_l, coordinate of the lth wall, m; x_{li}, coordinate of the lth wall of the ith section, m; α, heat transfer coefficient, W/(m^2·K); γ, adiabatic index; γ_i, adiabatic index in the ith section; γ_m, adiabatic index in the mth section; ΔT_i, temperature drop in the ith section, K; $\boldsymbol{\rho}$, gas-density matrix; ρ, gas density, kg/m^3; ρ_2, ρ_3, and ρ_4, gas densities in the 2nd, 3rd, and 4th sections, kg/m^3; ρ_m, gas density in the mth section, kg/m^3; ρ_{H1}, gas density in the 1st section at atmospheric pressure at height H, kg/m^3; μ, molar mass of gas, kg/mole; μ_1, μ_2, and μ_3, molar masses of gases in the 1st, 2nd, and 3rd sections, kg/mole; μ_i and μ_m, molar masses of gases in the ith and mth sections, kg/mole; $\boldsymbol{\sigma}$, wall section matrix; $\boldsymbol{\sigma}^*$, heat-transfer surface matrix; σ, section of one wall, m^2; σ^*, heat-transfer surface, m^2; σ_i, inner surface area of the ith section, m^2; σ_{ij}, part of the dm_i element surface on which p_i acts, m^2; σ_{ji}, part of the dm_i element surface in which p_j acts, m^2; τ, time of pass of the plate, sec; Ξ, separated area, m^2. Subscripts: 0, initial conditions; 01, initial parameters in the 1st section; ad, adiabatic; b, gap; fr1, friction in the 1st wall; fr2, friction in the 2nd wall; i, section number; in, internal; j, port number; k, source number; max, maximum value; n, nozzle; p, piston; p1, 1st piston; p2, 2nd piston; rad, radiation loss; t, thin-walled plate; d, before motion.

REFERENCES

1. J. A. Dowling, J. Shumsky, J. Eckerman, and R. E. Schelier, A demonstration of laser pumping using a compressed gas light source, *Appl. Phys. Lett.*, **12**, No. 5, 184–185 (1968).
2. A. D. Margolin, N. Ya. Vasilik, V. M. Shmelev, et al., Ballistic plasmatron as a source of UV radiation for photochemistry, in: *Ext. Abstr. of Papers presented at XVth Interbranch Sem. "Nuclear-Hydrogen Power Engineering and Technology"* [in Russian], Énergoatomizdat, Moscow (1990), pp. 58–61.
3. V. M. Shmelev, A. D. Margolin, N. Ya. Vasilik, V. G. Krupkin, T. V. Volov, and D. B. Volov, Ballistic plasmatron with a vortex chamber for pumping solid-state lasers, *Teplofiz. Vys. Temp.*, **36**, No. 4, 548–551 (1998).
4. A. D. Margolin, N. Ya. Vasilik, V. M. Shmelev, et al., Ballistic plasmatrons with multistage heating, in: *Ext. Abstr. of Papers presented at Ist All-Union Symp. on Radiative Plasmadynamics* [in Russian], Énergoatomizdat, Moscow (1989), pp. 33–34.
5. V. V. Kislykh and K. V. Krapivnoi, Use of nonisoentropic multistage compression for obtaining dense high-temperature gas, *Teplofiz. Vys. Temp.*, **28**, No. 6, 1195–1203 (1990).
6. D. B. Volov, *Heat Power Characteristics of the Vortex Chamber of a Ballistic Plasmatron*, Candidate Dissertation (in Engineering), Moscow (1989).
7. D. B. Volov and V. M. Shmelev, Experimental studies of the vortex chamber, in: *Coll. of Sci. Papers of Young Scientists and Post-Graduate Students of Samara Institute of Transportation Engineers* [in Russian], Samara (1997), pp. 83–89.
8. G. N. Abramovich, *Applied Gas Dynamics* [in Russian], Nauka, Moscow (1976).
9. S. V. Makarychev, G. D. Smekhov, and M. S. Yalovik, Radiation and radiative cooling of xenon plasma behind the front of a strong shock wave, *Izv. Ross. Akad. Nauk, Mekh. Zhidk. Gaza*, No. 1, 155–162 (1992).
10. I. N. Bronshtein and K. A. Semendyaev, *Handbook on Mathematics for Engineers and Students of Higher Technical Schools* [in Russian], Nauka, Moscow (1986).